

Electron-Irradiation Damage-Rate Measurements in Aluminum*

H. H. NEELY AND WALTER BAUER

Atomics International, A Division of North American Aviation, Canoga Park, California

(Received 27 April 1966)

The resistivity increase upon electron irradiation near 8°K of aluminum was measured as a function of incident electron energy from 0.19 to 1.6 MeV. A value of the displacement threshold energy of 16 eV was determined by extrapolation of the damage-rate curve to zero damage production. A reasonable fit between the experimental and theoretical values of the displacement cross section was achieved with an effective threshold energy of 19 eV, a value of the Frenkel resistivity of $(1.32 \times 10^{-4} \text{ ohm cm})/(\text{fractional concentration})$, and a unit step-displacement function. The tailing off in the damage rate near threshold that has been observed in Cu, Au, and Pt is apparently absent in Al.

I. INTRODUCTION

PREVIOUS studies of defect-production rates in metals as a function of electron energy have concentrated mainly on the noble metals, with the exception of the work of Lucasson and Walker.¹ They measured defect-introduction rates in a variety of metals, including aluminum. They found that in aluminum satisfactory agreement between displacement theory and experiment could be achieved with an effective threshold energy $T_e = 32$ eV and a Frenkel resistivity of $3.4 \times 10^{-4} \Omega\text{-cm}$ per unit concentration of Frenkel pairs. In their work it was pointed out that because of the thickness of the samples (0.014 in.), the experimental results have to be viewed "with reserve, and a repetition of the experiment using thin foils would be desirable." In addition, their measurements extended down only to a maximum energy transfer, $T_m \approx 60$ eV, which is substantially above the threshold energy for defect production. Thus their data cannot be used to extrapolate to zero damage production.

Recently Mehner *et al.*² reported the displacement threshold energy in aluminum to be 16.5 ± 3 eV. They did not state whether this is an effective threshold energy (deduced by a comparison of experiment with theory) or an empirical threshold energy (deduced by extrapolation to zero damage production). Preliminary results of the present work were reported at the same time.³

In this work we present experimental damage-rate measurements in aluminum for values of T_m from 15 to 330 eV. These data are compared to the displacement theory with different values of the effective threshold energy and two multiple-displacement models. A description of the experimental procedure is given in Sec. II. The experimental results are presented in Sec. III. In Sec. IV the experimental results are compared

with displacement theory, and in Sec. V a discussion of the results is given.

II. EXPERIMENTAL PROCEDURE

A. Specimen Preparation

The starting material of the samples was 99.9999% stated purity United Mineral ingot. The sample material was machined from the ingot, etched, then rolled between tantalum sheets to the final thickness of 0.0008 in. The foil was then sheared to a width of approximately 0.02 in. and a length of 1 in. The thickness was chosen to minimize energy degradation of the incident electrons while passing through the foils, and at the same time to provide enough mechanical rigidity for spotwelding of potential leads. In order to convert resistance increases to resistivity increases, one must have a knowledge of the geometrical factor A/L . Here A is the cross-sectional area and L is the irradiated length. For this reason, potential leads consisting of 2-mil gold wires were spotwelded on some of the samples. The samples were then mounted on a sample holder similar to the one described elsewhere.⁴ After mounting the holder on either the vertical or horizontal cryostat (see below) the samples were resistance-annealed for $2\frac{1}{2}$ h at an average temperature of 300°C. The samples had typical residual resistivities of 2.1 to $2.5 \times 10^{-9} \Omega\text{-cm}$. We believe that these values may be influenced by the size of the material, since the larger diameter material had residual resistivities of $0.65 \times 10^{-9} \Omega\text{-cm}$.

B. Irradiation

A horizontal High Voltage Corp. 0.4-MeV Van de Graaff was used for the source of electrons below 0.5 MeV. The energy of this accelerator was calibrated in the positive mode using the threshold for the $C^{12}(d,n)N^{13}$ reaction at 328 KeV. The accelerator potential was stable to within ± 2 KeV. To achieve a uniform beam intensity at the sample a 0.00025-in. Al foil was used to scatter the beam about 5 in. from the sample.

The higher energy electrons were furnished by a 2-MeV in-house-built Van de Graaff-type generator.

* Based on work sponsored by the Metallurgy Branch, Division of Research, U. S. Atomic Energy Commission, under Contract AT-(11-1)-GEN-8.

¹ P. G. Lucasson and R. M. Walker, *Phys. Rev.* **127**, 485 (1962).

² A. S. Mehner, G. W. Iseler, H. I. Dawson, and J. W. Kauffman, *Bull. Am. Phys. Soc.* **10**, 690 (1965); *Phys. Rev.* **146**, 468 (1966).

³ W. Bauer, in *Lattice Defects and Their Interactions*, edited by R. R. Hasiguti (Gordon and Breach, Science Publishers, Inc. New York, 1966) (to be published).

⁴ A. Sosin and H. H. Neely, *Rev. Sci. Instr.* **32**, 922 (1961).

This irradiation facility has a double 60° beam-analyzing magnet calibrated at 1.66 MeV with the $\text{Be}^9(\gamma, n)\text{B}^8$ reaction. This system allows an energy spread of $\pm 5\%$. No intervening scattering foils were used in these sets of measurements. The electrons from both accelerators were measured and integrated with an Elcor Model 308 integrator; the estimated total error of the flux did not exceed 5%.

A horizontal cryostat was used for the irradiations below 0.5 MeV. The vertical cryostat for the 2.0-MeV accelerator is essentially the same as the one reported earlier by Sosin and Neely.⁴ Since no potential leads were used in the low energy irradiations in the horizontal cryostat the absolute value of the resistivity increase could not be determined accurately. Therefore we normalized the absolute value of the low-energy data to the high-energy data at 0.4 MeV. (The values of the slopes of the curves were in good agreement at the normalization point.) This procedure of normalization reflects our confidence in the damage-rate measurements obtained in the vertical cryostats on the 2-MeV accelerator.

During the irradiations the sample temperature never rose above 8°K, with current densities of $2.5 \mu\text{A}/\text{cm}^2$. The same current density was used in both irradiation facilities. Standard potentiometric methods were used for the resistance measurements. The uncertainty in the resistivity measurements was $\pm 2 \times 10^{-12} \Omega\text{-cm}$.

III. EXPERIMENTAL RESULTS

The resistivity increase per unit electron flux $d\rho/d\phi$ as a function of T_m (maximum energy that can be imparted to a lattice atom by an electron) is shown in Figs. 1 and 2. The value of $d\rho/d\phi$ is evaluated at each energy from the straight-line segments of the experimental-resistivity increase per unit electron flux. The value of T_m (in eV) may be obtained from the equation

$$T_m = (560.8/A)(\bar{E}/m_0c^2)[2 + \bar{E}/m_0c^2]. \quad (1)$$

Here, A is the atomic weight (26.98), \bar{E} is the average bombarding energy in MeV and $m_0c^2 = 0.511$ MeV.

The experimental data points in Figs. 1 and 2 include corrections for the degradation of the electron energy during traversal through the sample. The average energy \bar{E} of the bombarding electrons at a point midway in the aluminum foil is taken as

$$\bar{E} = E_i - \frac{1}{2}\alpha t, \quad (2)$$

where E_i is the incident electron energy, α is the energy loss per unit distance of the electron, and t is the thickness of the foil. The value of α was determined from the work of Katz and Penfold.⁵ Typically, the energy correction near threshold (converted into maximum energy transfer to the lattice atom,) is 1 eV. Above 1-MeV bombarding energy, the correction is

⁵ L. Katz and R. S. Penfold, *Rev. Mod. Phys.* **24**, 28 (1952).

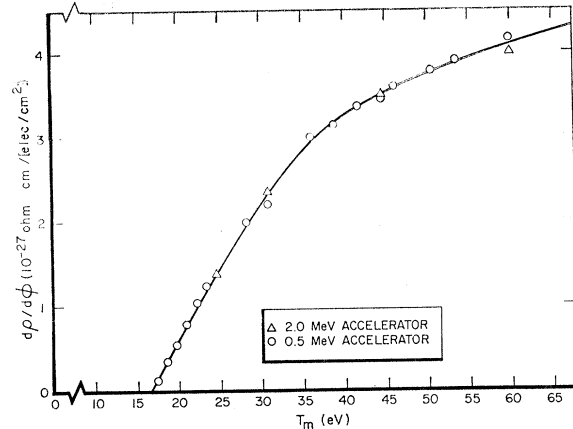


Fig. 1. The resistivity increase per unit electron flux as a function of the maximum energy transfer imparted a lattice atom T_m . The different experimental points from the 2.0 and 0.5-MeV accelerator were normalized as discussed in the text.

$\frac{1}{2}$ eV. The correction for electron straggling was also evaluated in the same manner as that of Sosin.⁶ The largest correction is near threshold and reduces the measured resistivity increment by only 3%. This correction is not shown in the data presented.

From the experimental data shown in Fig. 1 one can extrapolate the data to zero resistivity increase per unit flux with reasonable confidence. This yields a value of the threshold displacement energy $T_d = 16$ eV.

IV. COMPARISON OF EXPERIMENTAL RESULTS WITH DISPLACEMENT THEORY

The experimental values of $d\rho/d\phi$ may be compared with the theoretical values of the displacement cross section σ_d through the equation

$$d\rho/d\phi = \rho_F \sigma_d, \quad (3)$$

where ρ_F is the resistivity of a unit-concentration Frenkel pairs. Below we outline our calculation of σ_d . Since a considerable part of the electron-energy range is well in excess of the threshold energy, multiple displacements must be taken into account. The displacement cross section is defined as

$$\sigma_d(T_m) = \int_0^{T_m} P(T) \nu(T) \frac{d\sigma(T)}{dT} dT. \quad (4)$$

$P(T)$ is the probability of displacement of a lattice atom if an energy T is transferred to it, T_e is an effective threshold energy, $\nu(T)$ is the number of displaced atoms per primary knock-on (including the primary knock-on) and $d\sigma(T)/dT$ is the differential energy transfer cross section for electrons to a lattice atom, given by Seitz and Koehler.⁷

⁶ A. Sosin, *Phys. Rev.* **126**, 1698 (1962).

⁷ F. Seitz and J. S. Koehler, in *Solid State Physics*, edited by F. Seitz and D. Turnbull (Academic Press Inc., New York, 1956), Vol. II, p. 330.

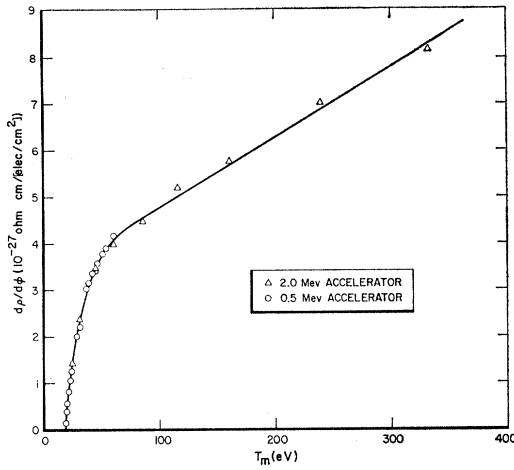


FIG. 2. The resistivity increase per unit electron flux as a function of the maximum energy transfer imparted a lattice atom T_m . The different experimental points from the 2.0- and 0.5-Mev accelerators were normalized as discussed in the text.

In this calculation we make the assumption of a unit-step probability of displacement:

$$P(T) = 0 \quad \text{for } T < T_e, \quad (5)$$

and

$$P(T) = 1 \quad \text{for } T \geq T_e.$$

We use two multiple-displacement models, both based essentially on the Kinchin and Pease⁸ formulation. This formulation embodies the following assumptions: (a) A struck atom is displaced only if it receives an energy greater than T_e . (b) The striking atom will remain at the collision site if the struck atom receives an energy larger than T_e but the striking atom is left

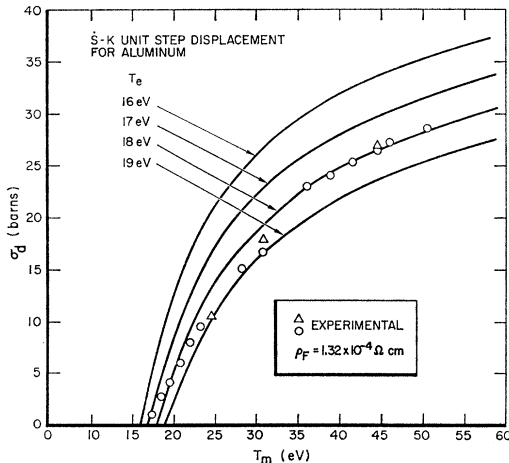


FIG. 3. The theoretical and experimental values of the displacement cross section σ_d as a function of the maximum energy transfer imparted a lattice atom T_m . The theoretical σ_d was calculated from the Seitz and Koehler (S-K) theory with unit displacement probability at T_e . The experimental σ_d was calculated from Eq. (3) of the text with the indicated value of the Frenkel resistivity ρ_F .

⁸ G. H. Kinchin and R. S. Pease, Rept. Progr. Phys. 18, 1 (1955).

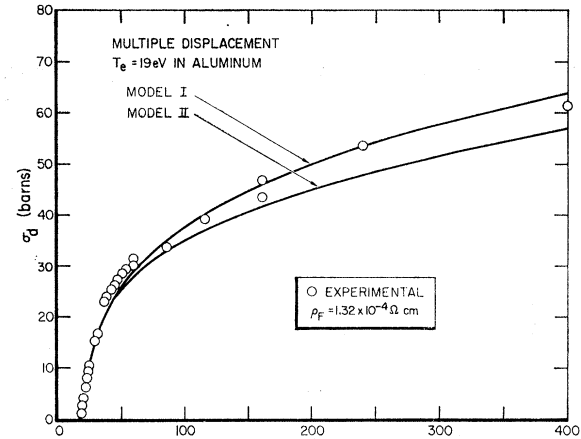


FIG. 4. The theoretical and experimental values of the displacement cross section σ_d as a function of the maximum energy transfer imparted a lattice atom T_m . The theoretical σ_d was calculated from a multiple-displacement theory in the text for a fixed value of T_e . [See Eq. (6) for model I and Eq. (7) for model II.] The experimental σ_d was calculated from Eq. (3) of the text with the indicated value of the Frenkel resistivity ρ_F .

with energy less than T_e . (c) A secondary struck atom does not lose an energy T_e when it is displaced.

Our two models differ only in the treatment of the primary knock-on. In the first model the primary recoil does not lose an energy T_e (see the treatment by Dienes and Vineyard⁹) and in the second model the primary recoil is assumed to lose an energy T_e (see Lucasson and Walker¹).

With these assumptions we have for model I

$$\sigma_d = \int_{T_e}^{T_m} \frac{d\sigma(T)}{dT} dT \quad \text{for } T_e < T_m < 2T_e \quad (6a)$$

and

$$\sigma_d = \int_{T_e}^{2T_e} \frac{d\sigma(T)}{dT} dT + \int_{2T_e}^{T_m} \frac{T}{2T_e} \frac{d\sigma(T)}{dT} dT \quad \text{for } T_m \geq 2T_e, \quad (6b)$$

and for model II

$$\sigma_d = \int_{T_e}^{T_m} \frac{d\sigma(T)}{dT} dT \quad \text{for } T_e < T_m < 3T_e \quad (7a)$$

and

$$\sigma_d = \int_{T_e}^{3T_e} \frac{d\sigma(T)}{dT} dT + \int_{3T_e}^{T_m} \frac{1}{2} \left[\frac{T}{T_e} - 1 \right] \frac{d\sigma(T)}{dT} dT \quad \text{for } T_m \geq 3T_e. \quad (7b)$$

The integrated expressions may be found in the Appendix.

⁹ G. J. Dienes and G. H. Vineyard, *Radiation Effects in Solids* (Interscience Publishers, Inc., New York, 1957), p. 28.

In Figs. 3 and 4 are shown the results of the cross-section calculations and the experimental values of the cross section as calculated by the use of Eq. (3) with an appropriate choice of ρ_F . In Fig. 3 we show the results of the calculation for the cross section without incorporating multiple displacements and for several values of T_e . The data seem to fall between the cross sections calculated for values of T_e of 18 or 19 eV. In Fig. 4 the displacement cross section was calculated for one value of T_e (19 eV) and the two multiple-displacement models. Again the data seem to fit reasonably well to the theory.

V. DISCUSSION

In fitting the theoretical and experimental values of σ_d to each other, one has essentially two adjustable parameters: T_e and ρ_F . The uncertainty in the experimental data near threshold limit the value of T_e usually to within a few eV of the value of T_d . One would expect the value of T_e (18–19 eV) to be a few eV above the value of T_d (16 eV) since $P(T)$ should reach unity above the minimum energy for displacement, T_d . The absolute value of σ_d changes by approximately 20% for a change of 2 eV in the value of T_e . Therefore, the value of ρ_F , derived by our comparison of experimental and theoretical results and within the assumptions inherent in the calculations, should be considered accurate to approximately 20%.

Our data fit the model I multiple-displacement theory best. However, in the light of the above-mentioned uncertainties, one should interpret the data merely as evidence that a Kinchin-and-Pease⁸-type multiple-displacement theory is adequate to energies of $T_m \approx 20T_d$.

In Fig. 1 one notes that there is no tailing-off in the $d\rho/d\phi$ curve near threshold such as is observed in gold,¹⁰ copper,¹⁰ and platinum.³ The reason for the absence of this tail in the damage-rate curve has been discussed in detail by one of the authors³ (W.B.). Essentially, the tail in the damage rate near threshold is most probably due to the displacement of light substitutional impurity atoms or of host atoms near such impurity atoms by focussons.¹⁰ The importance of these indirect-displacement processes depends on the efficiency of focussing and the concentration of light substitutional impurities. A crude measure of the focussing efficiency is the ratio of the nearest-neighbor distance to the Pauling ionic diameter, S/D , (2.86 for Al). Within the simple hard-sphere picture, defocussing occurs if $S/D > 2$. Thus, indirect displacements are not expected to be of importance in Al, as evidenced in the absence of the tail in the damage-rate curve.

When the experimental measurements of $d\rho/d\phi$ are compared with the theoretical value of the displacement cross section in Eq. (3), a value of ρ_F is determined. It is generally assumed that $\rho_F = \rho_i + \rho_v$, where ρ_i is the

resistivity of a unit concentration of interstitials and ρ_v is the resistivity of a unit concentration of vacancies. The best value of ρ_F deduced in the last section is $1.32 \times 10^{-4} \Omega\text{-cm}$. Simmons and Balluffi¹¹ have, by a comparison of high-temperature length and lattice-parameter measurements with the difference between the measured high-temperature resistivity and the calculated lattice contribution to the resistivity, deduced a value of $\rho_v = 3 \times 10^{-4} \Omega\text{-cm}$. Thus the value of ρ_F , as deduced in our measurements, is anomalously low.

This same dilemma was found to exist for gold by Bauer and Sosin,¹² who discussed the problem in some detail. They concluded, mainly on the basis of an empirical interatomic potential in gold, that the assumption of unit-displacement probability was too large because near threshold, displacements are possible only into a small solid angle about the (100) direction. This, of course, has the same effect as choosing a larger value of ρ_F in Eq. (3). We suggest that, because of the open lattice structure of Al (see above value of $S/D = 2.86$), the displacement energy should be relatively independent of the displacement direction (isotropic threshold energy surface).

The computer calculations of Domingos¹³ on aluminum have a bearing on this discussion. Domingos calculated several dynamic events, in the fashion of the Brookhaven group,¹⁴ with a modified Morse potential. He concluded that the threshold energy in the (100) direction is 20 eV and in the (110) direction, 25 eV. These values are in good agreement with the present experimental values of the threshold energy and furthermore suggest that the threshold-energy surface is isotropic.

An additional argument for isotropy lies in the nature of the data themselves. One notes that the agreement between theory (cross section) and experiment ($d\rho/d\phi$) for the same low value of ρ_F extends from near threshold to energies of approximately $3T_d$. (We exclude the multiple-displacement region in this argument.) This implies directly that there is no appreciable variation in the probability of displacement function [$P(T)$] over this energy range. If the threshold-energy surface were anisotropic, as was suggested in gold, $P(T)$ would increase for increasing energies as displacements into directions previously energetically unfavorable takes place. The fact that the value of T_e is only a few eV above that of T_d provides additional evidence that the threshold-energy surface is isotropic.

The value of ρ_F deduced here is based only on resistivity measurements. A more desirable method for deducing a value of ρ_F consists of the concurrent measurement of a number of physical parameters such as length change and stored energy upon irradiation.

¹¹ R. O. Simmons and R. W. Balluffi, *Phys. Rev.* **117**, 62 (1959).

¹² W. Bauer and A. Sosin, *Phys. Rev.* **135**, A521 (1964).

¹³ H. Domingos, University of Washington thesis, (unpublished).

¹⁴ J. B. Gibson, A. N. Goland, M. Milgram, and G. H. Vineyard, *Phys. Rev.* **120**, 1229 (1960).

¹⁰ W. Bauer and A. Sosin, *J. Appl. Phys.* **35**, 703 (1964).

tion and recovery. The Munich group¹⁵ has recently reported measurements of this type on aluminum after neutron irradiation. They deduced a value of $\rho_F = 3.3 \times 10^{-4} \Omega\text{-cm}$.

In the following discussion we consider a possible explanation for the anomalously low value of ρ_F after electron irradiation and the somewhat larger value of ρ_F after neutron irradiation. Since the mean-energy transfer to a primary knock-on is considerably larger for a neutron than for an electron, the mean distance for a Frenkel pair after electron irradiation is smaller than after neutron irradiation. If the scattering of conduction electrons by a Frenkel pair is subject to interference or strongly depends on the relaxation of the atoms surrounding the interstitial, one would expect the value of ρ_F to depend on the separation of the Frenkel pair. Overhauser and Gorman¹⁶ have calculated the resistivity of an interstitial atom in the copper lattice and found that approximately 90% of the value of ρ_i is due to the scattering of the relaxed atoms surrounding the interstitial. It is therefore conceivable that the value of ρ_i is considerably reduced in a close-pair configuration if the proximity of a vacancy alters the relaxation of the atoms surrounding the interstitial. This conclusion reached here for Al on the basis of a calculation for Cu may be subject to considerable modification because of the difference in the relaxations of the atoms and the different valence of the two metals. Some experimental evidence for interference effects in Al may be found in the early stages of Guinier-Preston zone formation.¹⁷

In this discussion we have indicated that the threshold energy surface in aluminum is probably largely isotropic. Thus the assumption of unit-step displacement probability at T_e is a good approximation. The displacement cross section calculated with this assumption was found to agree reasonably well with the experimental data for a value of $\rho_F \approx 0.4 \rho_v$. A possible explanation for this ρ_F anomaly involving electronic effects was considered.

There may be other factors which influence the quantities in Eq. (3) in such a way that agreement between theory and experiment can be achieved with a plausible value of ρ_F . In any case, it is clear that

¹⁵ H. Wenzl, W. Schilling, and K. Isebeck, *International Conference on Electron Diffraction and Crystal Defects, Melbourne, 1965* (Australian Academy of Science, Melbourne, 1965).

¹⁶ A. W. Overhauser and R. L. Gorman, *Phys. Rev.* **102**, 676 (1956).

¹⁷ See for example: H. Herman, J. B. Cohen, and M. E. Fine, *Acta Met.* **11**, 43 (1963) and other references therein.

further work is needed to understand fully the displacement process in aluminum.

ACKNOWLEDGMENTS

The authors wish to thank Dr. A. Sosin, Dr. D. W. Keefer, and Dr. K. Thommen for many fruitful discussions.

APPENDIX

In this section we present the integrated expressions for the theoretical displacement cross sections of Eqs. (6) and (7).

For the simple unit-step-function displacement probability and no multiple displacements the theoretical displacement cross section is,⁷

$$\sigma = A \left[\left(\frac{T_m}{T_e} - 1 \right) - \beta^2 \ln \left(\frac{T_m}{T_e} \right) + \pi\alpha\beta \left\{ 2 \left[\left(\frac{T_m}{T_e} \right)^{1/2} - 1 \right] - \ln \left(\frac{T_m}{T_e} \right) \right\} \right], \quad (\text{A1})$$

where $A = 2.5 \times 10^{-25} Z^2 (1 - \beta^2) / \beta^4$ (cm²).

For the Model I multiple-displacement theory the cross section for $T_m \geq 2 T_e$ is

$$\sigma = A \left\{ \frac{T_m}{2T_e} \left[1 + \ln \left(\frac{T_m}{2T_e} \right) \right] - \beta^2 \left(\frac{T_m}{2T_e} - 0.3069 \right) + \pi\alpha\beta \left[0.3069 - 1.172 \left(\frac{T_m}{2T_e} \right)^{1/2} + \frac{T_m}{2T_e} \right] \right\}. \quad (\text{A2})$$

For the Model II multiple displacement theory the cross section for $T_m \geq 3 T_e$ is

$$\begin{aligned} \sigma = A \left\{ \frac{2T_m}{3T_e} - (\beta^2 + \pi\alpha\beta) \ln 3 + 2\pi\alpha\beta \left[\left(\frac{T_m}{T_e} \right)^{1/2} - \left(\frac{T_m}{3T_e} \right)^{1/2} \right] \right. \\ \left. - \frac{1}{2} \left[\left(\frac{T_m}{3T_e} \right) - 1 - \beta^2 \ln \left(\frac{T_m}{3T_e} \right) + \pi\alpha\beta \left\{ 2 \left[\left(\frac{T_m}{3T_e} \right)^{1/2} - 1 \right] \right. \right. \right. \\ \left. \left. - \ln \left(\frac{T_m}{3T_e} \right) \right\} \right] + \frac{T_m}{2T_e} \left[\ln \left(\frac{T_m}{3T_e} \right) - \left(1 - \frac{3T_e}{T_m} \right) \right. \right. \\ \left. \left. \times (\beta^2 + \pi\alpha\beta) + 2\pi\alpha\beta \left[1 - \left(\frac{3T_e}{T_m} \right)^{1/2} \right] \right] \right\}. \quad (\text{A3}) \end{aligned}$$

Here $\alpha = Z/137$ and $\beta = v/c$.